

## GASES AND GAS HYDRATES IN THE EARTH'S CRYOSPHERE

METHOD OF RAPID ESTIMATION OF THE EFFECT  
OF THE HYDRATE-FORMING GAS PRESSURE  
ON NONCLATHRATED WATER CONTENT IN SOILSV.A. Istomin<sup>1,2,\*</sup>, D.V. Sergeeva<sup>2</sup>, E.M. Chuvilin<sup>2</sup>, B.A. Bukhanov<sup>2</sup>, N.S. Sokolova<sup>2</sup><sup>1</sup> Gazprom VNIIGAZ LLC, Malokhtinsky prosp. 45A, St. Petersburg, 195112 Russia<sup>2</sup> Center for Petroleum Science and Engineering, Skolkovo Institute of Science and Technology, Bolshoi Boulevard 30/1, Moscow, 121205 Russia

\*Corresponding author; e-mail: vlistomin@yandex.ru

Natural gas hydrates exist in porous media at high pressure and low temperature, including permafrost. The development of express methods for calculating hydrate phase equilibria in soils and sediments, including the equilibrium content of nonclathrated water, i.e., the pore water, which is in equilibrium with hydrate and hydrate-forming gas under given thermobaric conditions, is of special interest in the study of natural hydrates. Nonclathrated water is similar to unfrozen water in frozen soils. The current study covers thermodynamic relationships for calculating nonclathrated water content in soil under certain thermobaric conditions on the basis of experimental data of pore water activity and soil water content. It is shown that at a fixed temperature the nonclathrated water content sharply decreases according to a power law during an increase in gas pressure. The results of thermodynamic calculation are in agreement with direct measurements of nonclathrated water in soil systems using the contact method. Thus, at temperatures below 0°C, the content of nonclathrated water in kaolinite clay and in sandy clayey soils decreases by more than two times with an increase in methane pressure from 2.3 to 11 MPa. The obtained relationships allow us to recalculate the nonclathrated water content upon transition from one hydrate-forming gas to another, as well as calculate nonclathrated water content using the unfrozen water content curve at different temperatures. The developed thermodynamic approach can be applied to various hydrate-forming gases and their mixtures.

**Keywords:** gas hydrates, sediments, pore water, phase equilibria, nonclathrated water, unfrozen water, ice, thermodynamic calculations.

**Recommended citation:** Istomin V.A., Sergeeva D.V., Chuvilin E.M., Bukhanov B.A., Sokolova N.S., 2024. Method of rapid estimation of the effect of the hydrate-forming gas pressure on nonclathrated water content in soils. *Earth's Cryosphere* XXVIII (4), 33–43.

## INTRODUCTION

The effect of porous media on phase equilibria of gas hydrates has been studied in Russia since the 1960s. The first experimental data obtained by Yu.F. Makogon [Makogon, 1974] showed that thermobaric equilibrium conditions of hydrate formation in a porous medium may differ from those of hydrate formation in a free volume. To evaluate the influence of different types of porous media, including dispersed soils, on gas hydrate equilibria, a new parameter – the capillary radius – was added to the thermodynamic model under the assumption that the porous medium can be described as a system of capillaries with a certain average radius. As a rule, for hydrophilic capillaries, the value of  $\cos \theta$  was assumed to be equal to unity ( $\theta$  is the contact angle). Such a simple model allowed us to calculate the value of the temperature shift of the hydrate formation curve at a given pressure depending on the average radius of capillaries, in which the pore water is located. The

hydrate formation temperature shift increases with decreasing capillary radius. A further step in the description of hydrate equilibria in a porous medium was to define the structure of the pore space of the soil system as a certain distribution (from narrow to wide) of capillaries by size. Using this distribution, it is possible to determine the thermodynamic properties of pore water, to calculate the shift of hydrate equilibrium from the sample moisture content, and to compare the calculations with direct experimental measurements [Handa, Stupin, 1992; Clarke et al., 1999; Uchida et al., 1999, 2002, 2004; Klauda, Sandler, 2001; Melnikov, Nesterov, 2001; Wilder et al., 2001; Seo et al., 2002; Smith et al., 2002, 2004; Anderson et al., 2003; Kang et al., 2008; Li et al., 2008; Chen et al., 2010; Lee, Seo, 2010]. In our opinion, this approach is mainly of methodological importance [Istomin et al., 2015] because of the incomplete correspondence of the model of size-distributed capillaries to real soil

systems, as well as because of the imperfection of the methodology of direct experimental measurement of hydrate equilibrium shift in a pressure chamber. However, for specially prepared model porous media with artificially obtained capillaries and their very narrow size distribution, this approach turns out to be quite acceptable [Uchida et al., 1999; Istomin et al., 2015a, 2017b].

It is important to note that in a simple capillary model, the hydrate equilibrium shift does not depend on the moisture content of the porous media sample (in a wide range of moisture contents), which is clearly not the case for real soil systems. This seems quite obvious, based on the analogy with unfrozen water: the content of unfrozen water in a sample is a function of temperature, since the temperature shift of the ice–pore water phase equilibrium is determined by the water content in the sample. Therefore, by analogy with the concept of unfrozen water in permafrost soils, a new concept of nonclathrated water in the ground system, which is in equilibrium with gas hydrate and hydrate-forming gas under given thermobaric conditions, was introduced [Chuvilin et al., 2011; Chuvilin, Istomin, 2012].

The content of nonclathrated water in hydrate-saturated porous media depends on a number of factors: pressure, temperature, gas composition, and pore water mineralization. Note that, unlike unfrozen water, the concept of nonclathrated water applies to both negative (subzero) and positive (above-zero) temperatures. Also, like unfrozen water in frozen soils, nonclathrated water can have a significant impact on the physical, chemical, and mechanical properties of frozen and hydrate-bearing reservoirs. Currently, the term “nonclathrated water” is already actively used in the references [Hansen et al., 2016; Sell et al., 2018; Yakushev, 2019].

As for the experimental determination of the hydrate equilibrium shift in porous media, the traditional approach is to study this equilibrium in a hydrate chamber depending on the moisture content of samples, similar to the study of hydrate equilibria in the free volume. It should be emphasized that, in order to obtain more or less reliable results, it is necessary to overcome a number of technical difficulties associated with obtaining hydrates directly in a porous medium (the experiment technique is described in [Uchida et al., 2004]), while the accuracy of measurements remains not very high. At present, the traditional technique of studying hydrate equilibria in porous media continues to be developed [Chuvilin et al., 2010; Chong et al., 2016; Zarifi et al., 2016; Liu et al., 2018; Park et al., 2018; Zhou et al., 2019; Em et al., 2020; Zhang, Taboada-Serrano, 2020; Azimi et al., 2021; Liang et al., 2021; Zaripova et al., 2021]. However, in our opinion, it is difficult to guarantee precise results within its framework.

A fundamentally new approach to the experimental study of nonclathrated water content in real soil systems was developed in our works [Chuvilin et al., 2008, 2010a,b] by analogy with the contact method for determining unfrozen water in a water-saturated soil system. The method for determining the content of nonclathrated water, i.e., pore water in a dispersed medium in equilibrium with gas hydrate, is as follows. A pre-dried and weighed sample of dispersed medium is placed between two plates of ice or ice-containing soil in direct contact with them, and then the sample together with the plates of ice or ice-containing soil is placed in a pressure chamber at a specified subzero temperature. A hydrate-forming gas is injected to a pressure exceeding the pressure of the three-phase ice–gas–hydrate equilibrium. The sample is maintained in the pressure chamber until it reaches equilibrium saturation with water. Then, the gas pressure in the chamber is reduced to atmospheric pressure. The sample is removed and weighed. The difference in the sample mass before and after the experiment is used to determine the equilibrium water content in the sample. The uniqueness of this approach is that the soil initially contacts an ice plate rather than a hydrate plate, but the equilibrium of pore water with the hydrate is studied at a specified hydrate-forming gas pressure. This is explained by the fact that the ice surface in the pressure chamber is covered with a hydrate film, so saturation of the porous medium with pore water takes place only until equilibrium with the hydrate is reached. It should be emphasized that we have implemented the proposed method not only at subzero temperatures but also, with some modifications, at positive temperatures.

It should be noted that the developed method for determining nonclathrated water in hydrate-containing porous media is rather labor-intensive and time-consuming: the experiment can last several weeks, which is also typical for the contact method for determining unfrozen water. Therefore, for soil systems it is worthy of attention and development of a more rapid approach, in which thermodynamic properties of pore water (activity) are directly measured depending on its content in the soil sample. And the obtained data on pore water activity in samples depending on their moisture content allow further thermodynamic calculations of pore water content at equilibrium not only with ice (see works on the express method of determining the curve of unfrozen water [Chuvilin et al., 2008, 2010b, 2018, 2020; Istomin et al., 2017a]) but also with gases and gas hydrates.

The described approach is developed below for phase equilibria of gas hydrates with pore water of water saturated soil systems. Initially, it was developed to determine the temperature shift of hydrate equilibrium at fixed pressure [Istomin et al., 2009,

2015b; Chuvilin, Istomin, 2012]. These works considered in detail the temperature shift of hydrate equilibrium  $\Delta T$  at constant pressure as a function of sample moisture content and pore water activity using numerical calculation methods, without explicitly writing out analytical thermodynamic relations. Whereas the main task of the present work is to obtain analytical thermodynamic relationships for the influence of hydrate-forming gas pressure on the pore (nonclathrated) water content in a sample in equilibrium with gas hydrates at a given temperature. In this case, the gas pressure  $P$  should be greater than  $P_{eq}$  – the pressure of hydrate formation corresponding to the equilibrium of gas hydrate with bulk water (or ice) at the considered temperature.

### Estimation of the influence of hydrate gas pressure on the nonclathrated water content

To describe the thermodynamic properties of pore water, we will use the water activity  $a(T, W)$ , which depends on the water content of the sample and temperature:

$$a = \frac{P_{wpor}}{P_w}, \quad (1)$$

where  $P_{wpor}$  is the water vapor pressure over the sample with water content  $W$  (wt. % of water relative to dry sample), and  $P_w$  is the pressure of saturated water vapor over bulk water (in MPa or Pa).

Experimental determination of pore water activity  $a(T, W)$  as a function of water content  $W$  in the soil (in % of dry sample) at room or near room temperature and atmospheric pressure can be carried out by various methods. The most rapid method is to measure the dew point temperature of air at atmospheric pressure equilibrated with a water-containing soil sample and then convert to pore water activity.

The methodology of pore water activity measurement in water saturated systems is described in detail in [Chuvilin *et al.*, 2020, 2022]. The activity is determined using WP4 type instruments developed by Decagon Devices (USA). For this purpose, soil samples with a given moisture content are placed in the measuring cup of the device (with internal dimensions: diameter 3.8 cm, height 1.0 cm). After the initial determination of water activity in the soil sample, a step-by-step drying of the soil sample is carried out, followed by activity measurement. In general, it is recommended to perform at least six–seven activity measurements on a soil sample at different moisture values. The time required for one measurement in WP4 instruments is usually about 30 min.

The pore water activity in a wet sample ( $a$ ) depends on both the water content of the sample and its temperature. However, as a first approximation, the dependence of pore water activity on temperature (at a fixed moisture content  $W$ ) can be neglected. However, this assumption becomes not quite valid for

small values of moisture content  $W$  of the porous media, especially in the presence of a clay component with a sliding framework (i.e., for the interlayer form of bound water).

The content of nonclathrated water, in contrast to unfrozen water, as will be shown below, strongly depends on vapor pressure. Whereas with increasing vapor pressure, the unfrozen water content in a frozen soil sample at a fixed subzero temperature increases only slightly. In this case, unfrozen pore water (in equilibrium with ice) is considered only at pressure  $P$ , below the pressure  $P_{eq}$ , which corresponds to the vapor–ice–hydrate equilibrium. The methodology for calculating the effect of vapor pressure on the content of unfrozen water is discussed in detail in [Istomin *et al.*, 2018]. At pressure  $P$  greater than  $P_{eq}$ , hydrate becomes thermodynamically stable phase instead of ice. Thus, the liquid phase at the pressure of hydrate-forming gas  $P > P_{eq}$  should be considered already as nonclathrated water. From general thermodynamic considerations it follows that at constant temperature the amount of nonclathrated water in the soil sample decreases with increasing pressure of hydrate-forming gas (because part of pore water at increasing pressure passes into the hydrate phase).

The areas of existence of unfrozen and nonclathrated water in dispersed sediments are shown in Fig. 1. The lines of three-phase gas–water/ice–hydrate equilibria are shown here. Above these lines is the zone of existence of nonclathrated pore water in water saturated soil systems, and below the VIH line is the zone of unfrozen water at subzero temperature.

The relationship between unfrozen and nonclathrated water content from gas pressure is shown in Fig. 2 for two fixed temperatures:  $t_1 < 0^\circ\text{C}$  и  $t_2 > 0^\circ\text{C}$ .

At temperature  $t < 0^\circ\text{C}$  ( $t_1$  in Fig. 2), the content of unfrozen water in the pore medium slightly in-

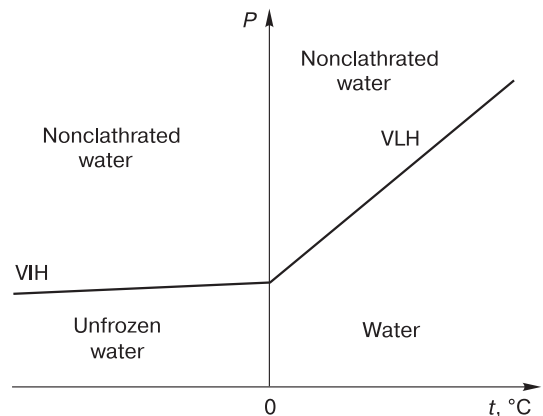


**Fig. 1. Regions of existence of nonclathrated and unfrozen water in dispersed rocks on the phase diagram of gas hydrates.**

Lines of three-phase equilibria: VIH – “vapor–ice–hydrate”; VLH – “vapor–water–hydrate”.

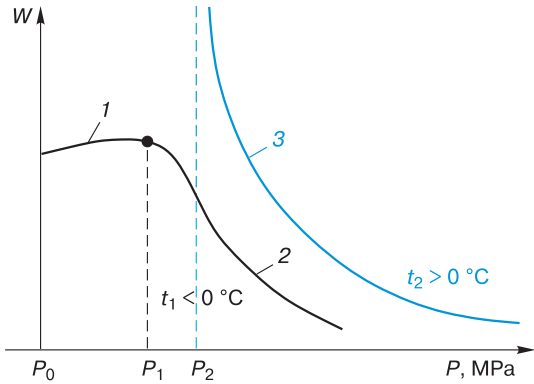


**Fig. 2. Equilibrium pore water content  $W$  in the soil system versus pressure  $P$  of hydrate-forming gas at  $P_0 = 0.1$  MPa.**

1 – unfrozen water at temperature  $t_1 < 0^\circ\text{C}$  to gas pressure  $P_1$ ; 2 – nonclathrated water at  $t_1 < 0^\circ\text{C}$  and gas pressure greater than  $P_1$ ; 3 – nonclathrated water at  $t_2 > 0^\circ\text{C}$  and gas pressure greater than  $P_2$ .

increases with increasing gas pressure. And the effect of increase of unfrozen water is quite small for  $\text{CH}_4$ , but it is much more significant for  $\text{CO}_2$  because of high solubility of  $\text{CO}_2$  in water. It should be considered for  $\text{N}_2$ , where it is possible to increase gas pressure up to ~14–15 MPa without nitrogen hydrate formation, as well as for mixtures of  $\text{CO}_2$  with  $\text{N}_2$ , because in addition to gas solubility in water, the total pressure in the system starts to influence the equilibrium “vapor–pore water”. When the pressure  $P_1 = P_{\text{eq}}$ , corresponding to the VIH equilibrium, is reached, a stable hydrate phase appears in the system (the quadrupole point “vapor–pore water–ice–hydrate” is reached). Further pressure increases lead to the disappearance of pore ice in the system (ice is transformed into hydrate), which corresponds to hydrate equilibrium with nonclathrated water, and the content of non-

clathrated water in the ground medium decreases with pressure increase according to the step law (see below the consideration of the corresponding analytical dependences).

At temperature  $t > 0^\circ\text{C}$  ( $t_2$  in Fig. 2), the picture changes: unfrozen water no longer exists in the ground medium, and nonclathrated water can exist only at vapor pressures  $P > P_2$  ( $P_2$  corresponds to the equilibrium pressure along the VLH line at temperature  $t_2$ ), since the equilibrium pore water content formally tends to infinity when approaching the VLH line. With increasing vapor pressure  $P$ , the content of nonclathrated water at  $t > 0^\circ\text{C}$  also decreases according to the power law.

Let us consider the pressure dependences of water activity  $a$  and nonclathrated water content  $W$  at positive and subzero temperatures.

For a given positive temperature at  $P = P_{\text{eq}}$  the value of activity  $a = 1$ , further at  $P > P_{\text{eq}}$  water activity  $a < 1$ , and with increasing vapor pressure pore water activity  $a$  decreases (Fig. 3a). At the same time, the content of nonclathrated water ( $W$ ) in the sample decreases according to the dependence shown in Fig. 2 (line 3 in Fig. 2).

For subzero temperature  $t$  (set point on line VIH, Fig. 1) and at  $P = P_{\text{eq}}$  the value  $a = a_{\text{eq}} < 1$ . With increasing pressure  $P$  at  $P > P_{\text{eq}}$ , the pore water activity  $a$  decreases (Fig. 3b). At the same time, the content of nonclathrated water ( $W$ ) in the sample decreases according to the qualitative dependence shown in Fig. 2 (line 2).

We proceed to the discussion of thermodynamic relations characterizing the activity and content of nonclathrated water from the pressure of the hydrate-forming gas.

In the work [Sergeeva et al., 2021], using the thermodynamic model of the Van der Waals–Platteu gas hydrate phase, a detailed derivation of approximate analytical thermodynamic relationships linking

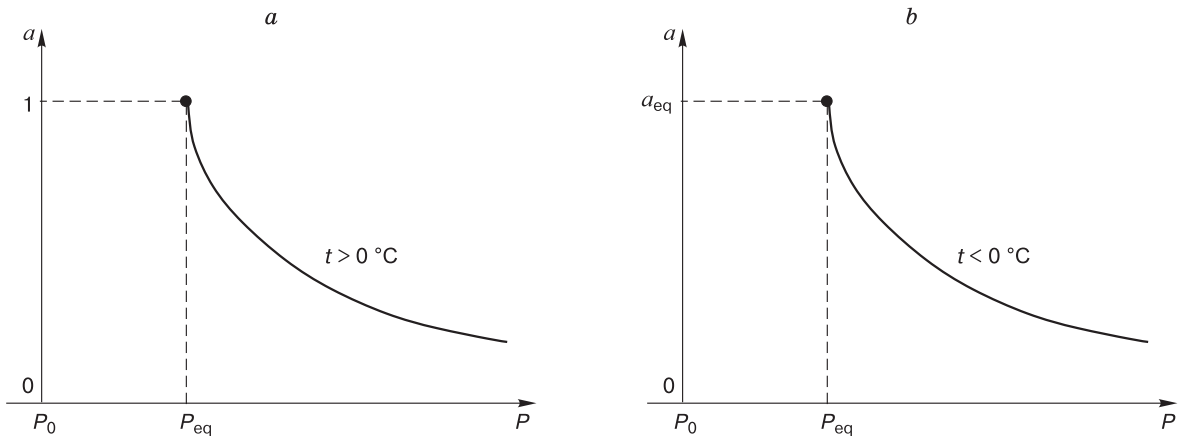


**Fig. 3. Activity of nonclathrated pore water  $a$  depending on the pressure of hydrate-forming gas at a fixed temperature:**

$a - t > 0^\circ\text{C}$ ;  $b - t < 0^\circ\text{C}$ ;  $P_0 = 0.1$  MPa.

the pore water activity ( $a$ ) in the soil system (measured at atmospheric pressure) with the fugacity/pressure of the hydrate-forming gas at a fixed temperature is presented. Positive and subzero temperatures are considered separately (at subzero temperatures the specificity of thermodynamic calculation arises due to the presence of unfrozen water). Below we present and analyze the approximate analytical relations obtained in [Sergeeva et al., 2021] with emphasis on a detailed discussion of their practical applicability.

Let us consider the effect of pressure of the hydrate-forming gas on the content of nonclathrated water at temperatures above 0°C (273.15 K). When analyzing thermodynamic relations, it is more convenient to set the temperature in Kelvin ( $T$ ), while in experiments it is more convenient to set the temperature in degrees Celsius ( $t$ ).

First of all, it is necessary to obtain experimental data on the dependence of pore water activity on the water content in the sample ( $W$ ), i.e., the dependence  $a = a(W)$  at atmospheric pressure. Then it is necessary to select a hydrate-forming gas (e.g., methane, CO<sub>2</sub>, ethane, propane, nitrogen, their mixtures, as well as natural gas).

The line of three-phase equilibrium “gas–bulk water–hydrate” is given by available experimental data, or calculated using some available software (e.g., HydroFLASH, Hydract Ltd). Many monographs on gas hydrates also provide similar analytical approximations of the lines of three-phase equilibria with water/ice for pure gases, e.g., [Istomin, Yakushev, 1992]. Let at the considered temperature  $T > 273.5$  K the pressure of hydrate formation (equilibrium with the bulk water phase) be  $P_{eq}$ , with the fugacity of the gas being  $f_{eq}$  and  $z_{eq}$  being its compressibility factor. We will assume that by means of measurements at atmospheric pressure the pore water activity in the studied soil sample  $a = a(W) < 1$  as a function of moisture content was experimentally obtained according to the methodology described in detail earlier [Chuvilin et al., 2020, 2022].

At pressure  $P < P_{eq}$ , hydrates are absent in the system (Fig. 1). At  $P = P_{eq}$ , the amount of nonclathrated water ( $W$ ) in the sample formally tends to infinity (Fig. 2). We are interested in thermodynamic relations between vapor pressure  $P$  at three-phase equilibrium “gas–pore water–hydrate”  $P \geq P_{eq}$ , pore water activity  $a(T, W) < 1$ , and water content in the sample ( $W$ ).

In [Sergeeva et al., 2021], the following approximate relations expressing the ratio of the gas fugacity  $f$  (at pressure  $P$  and pore water activity ( $a$ )) to the gas fugacity  $f_{eq}$  (at vapor pressure  $P_{eq}$  and water activity) were obtained  $a_{eq} = 1$ ):

$$\frac{f}{f_{eq}} = \left( \frac{b}{b_{eq}} \right)^{-n}, \quad (2)$$

$$b = a(1-x) \exp \left( -\frac{\Delta V_{hw}(P-P_0)}{RT} \right),$$

$$b_{eq} = a(1-x_{eq}) \exp \left( -\frac{\Delta V_{hw}(P_{eq}-P_0)}{RT} \right).$$

Here:  $b, b_{eq}$  – complex parameters;  $n$  – hydrate number;  $P_0 = 0.1013$  MPa;  $P$  and  $P_{eq}$  – respectively, the given vapor pressure and the pressure corresponding to the three-phase equilibrium with bulk water, MPa;  $a$  – water activity at the given moisture content ( $W$ ) of the sample measured at atmospheric pressure;  $x, x_{eq}$  – gas solubility, respectively, in pore water and in the bulk water phase at pressures  $P$ , mol. fraction;  $\Delta V_{hw}$  is the difference of molar volumes of water in hydrate and liquid water, and  $\Delta V_{hw} = 4.595$  и  $5.045$  cm<sup>3</sup>/mol for structures I and II, respectively;  $R$  is universal gas constant,  $R = 8.31446$  J/(K·mol).

In relations (2), the line of three-phase equilibrium “gas–bulk water phase–hydrate”, which is considered to be known, is used as a reference line. The gas fugacity ( $f$ ) can be determined by some equation of state. Since we are mainly interested in low pressures (up to 10 MPa), practically any equation of state, such as cubic equations, can be used to calculate the fugacity of a gas.

For the case of an ideal gas,  $f$  coincides with its pressure, i.e.,  $f = P$ . This means that at low pressures equation (2) can be approximated as follows:

$$\frac{P}{P_{eq}} = \left( \frac{b}{b_{eq}} \right)^{-n} = (a)^{-n}, \quad (3)$$

since in the first approximation  $b/b_{eq} \approx a$  (at low gas solubility in water and low pressures).

If the gas is weakly non-ideal (for example, for methane at pressures less than 7–8 MPa), then considering the approximate thermodynamic formula

$$f \approx z(P) \cdot P$$

relation (3) may be rewritten in the form

$$\frac{P}{P_{eq}} \approx \frac{z_{eq}}{z} \left( \frac{b}{b_{eq}} \right)^{-n} \approx \frac{z_{eq}}{z} (a)^{-n}, \quad (4)$$

where  $z = z(P)$ ,  $z_{eq} = z(P_{eq})$  are the gas compressibility factors at pressures  $P$  and  $P_{eq}$ , respectively.

It can be seen that in relation (4), instead of fugacity, the compressibility factor of the gas appears, so it is more convenient (although less accurate) for use in practical calculations.

From relations (3) and (4) follows a strongly nonlinear nature of the relationship between vapor pressure and pore water activity, with the equilibrium content of nonclathrated water falls sharply with increasing pressure of the hydrate-forming gas (accord-

ing to the power law with the exponent of degree close to the hydrate number  $n$ ).

Concerning the value of the hydrate number  $n$  in formulas (2), (3) and (4), we should note the following. For gases, in hydrate structures of which only large cavities are filled at  $T > 273.15$  K hydrate number  $n = 1/v_2$ , where  $v_2$  is a crystallochemical constant characterizing the number of large cavities in the hydrate structure. In this case, the large cavities are almost completely filled, the degree of their filling  $\theta_2$  is very close to unity, i.e., for propane and isobutane  $n \approx 17$ , since  $v_2 = 1/17$ , and for ethane  $n \approx 7.67$ , since  $v_2 = 3/23$ . Whereas for methane and nitrogen, when both types of hydrate cavities are strongly filled,  $n = 1/v_1 + 1/v_2$  for these hydrates at pressures close to  $P_{eq}$  is close to 6, and with increasing pressure tends to the limiting values of 5.75 and 5.67, respectively. At the same time, for  $\text{CO}_2$  hydrate, the hydrate number varies (due to incomplete filling of the small cavity in the hydrate structure) depending on the vapor pressure in wider ranges. Therefore, when performing accurate calculations in formulas (2), (3) and (4), it is necessary to consider some change (decrease) of the hydrate number with increasing pressure. In this case, the calculation can be carried out and “by pressure steps”, setting first  $n$  on the line of three-phase equilibrium with the volume phase of water (or ice, see below) and changing it at each step, aiming at the limit value  $\theta_1$ , equal to 1. For such a calculation,  $\theta_1$  can be estimated by the approximate relation

$$\theta_1 \approx \beta \frac{f_{eq}}{f} \approx \beta \frac{z_{eq} P_{eq}}{z P}, \quad (5)$$

where  $\theta_1$  is the degree of filling of a small cavity in the hydrate structure, and  $\beta$  is the proportionality parameter (which is calculated from the known value of the hydrate number ( $n_{eq}$ ) on the three-phase equilibrium line when the degree of filling of large cavities is set equal to one). This calculation scheme is almost identical to the calculation by the thermodynamic model of van der Waals–Platteeu, but it is more illustrative and allows us to use reliable correlations from experimental data for the reference curves of three-phase equilibrium, if necessary.

Let us further consider thermodynamic relations for calculating the content of nonclathrated water at temperatures below 273.15 K. Formally it is possible to apply relations (2), (3) and (4) for this temperature range, but it should be borne in mind that in this case the line of three-phase equilibrium “gas–bulk supercooled water–hydrate” as a continuous continuation of the line “gas–bulk water–hydrate” to the region of subzero temperatures will be used as a reference line (reference line). It should be noted that experimental data on such lines of three-phase metastable equilibrium were first obtained in the works of [Melnikov *et al.*, 2010, 2011].

It should be noted that for a given subzero temperature in the pressure range between the equilibrium pressure with supercooled water volume phase  $P_{eq}^{liq}$  and the equilibrium pressure with ice volume phase  $P_{eq}^{ice}$ , unfrozen water is physically realized in the pore medium (since there is no hydrate phase). Consequently, for such pressure range by formulas (2), (3) and (4) at subzero temperature the metastable nonclathrated water content is calculated as ice was absent in this temperature range, which is not physically realized in water saturated soil groundwater systems.

Thus, calculations of nonclathrated water content at subzero temperatures should be performed only for pressures  $P > P_{eq}^{ice}$  (when there is no more ice in the soil system because pore ice is replaced by thermodynamically more stable hydrate phase). As a reference line at subzero temperatures, it is preferable, in our opinion, to use the line of three-phase equilibrium “gas–bulk ice phase–hydrate”. The advantage of this reference line is that in the practically significant temperature range from  $-15$  to  $0^\circ\text{C}$ ,  $n$  along this line changes insignificantly (Table 1).

Using the VIH equilibrium as a reference line, the following thermodynamic relation was obtained in [Sergeeva *et al.*, 2021]:

$$\frac{f_{eq}}{f_{eq}^{ice}} = \left( \frac{b_{eq}^{ice}}{b_{eq}} \right)^{-n}, \quad (6)$$

$$b^{ice} = a(1-x) \exp\left( -\frac{\Delta V_{hi}(P-P_0)}{RT} \right), \quad a < a_{eq},$$

$$b_{eq}^{ice} = a_{eq}(1-x_{eq}) \exp\left( -\frac{\Delta V_{hi}(P_{eq}-P_0)}{RT} \right).$$

Here  $\Delta V_{hi} = V_h - V_i = 2.96$  and  $3.41$   $\text{cm}^3/\text{mol}$ , respectively, for hydrates of cubic structures I and II.

At low vapor pressures instead of equation (6) we can use the relation

$$\frac{P}{P_{eq}^{ice}} \approx \frac{z_{eq}}{z} \left( \frac{b_{eq}^{ice}}{b_{eq}} \right)^{-n}. \quad (7)$$

And for the case of an ideal gas:

$$\frac{P}{P_{eq}^{ice}} \approx \left( \frac{b_{eq}^{ice}}{b_{eq}} \right)^{-n} \approx \left( \frac{a_{eq}^{ice}}{a_{eq}} \right)^{-n}. \quad (8)$$

An important difference between relation (6) and relation (2) is the appearance of a new quantity  $a_{eq}$ , which is included in the definition of  $b_{eq}^{ice}$ .

The value  $a_{eq}$  corresponds to the equilibrium “ice – unfrozen water” for the soil system at atmo-

Table 1. Hydrate numbers and filling degrees for some gas hydrates on the equilibrium lines VIH (vapor–ice–hydrate) and VLH (vapor–water–hydrate)

Hydrate-forming gas		VIH equilibrium line, $t < 0^\circ\text{C}$			VLH equilibrium line, $t \geq 0^\circ\text{C}$			
		-15	-10	-5	0	5	7	10
Methane	$n_{\text{eq}}$	6.01	6.03	6.04	6.05	5.98	5.96	5.93
	$\theta_1$	0.89	0.89	0.88	0.88	0.90	0.91	0.93
	$\theta_2$	0.99	0.98	0.98	0.98	0.98	0.98	0.99
Ethane	$n_{\text{eq}}$	7.75	7.76	7.76	7.77	7.74	7.73	7.72
	$\theta_2$	0.99	0.99	0.99	0.99	0.99	0.99	0.99
Propane	$n_{\text{eq}}$	~17	~17	~17	17	17	–	–
	$\theta_2$	~1	~1	~1	~1	~1	–	–
Isobutane	$n_{\text{eq}}$	~17	~17	~17	17	–	–	–
	$\theta_2$	~1	~1	~1	~1	–	–	–
Nitrogen	$n_{\text{eq}}$	6.19	6.21	6.23	6.18	5.99	–	–
	$\theta_1$	0.88	0.87	0.87	0.88	0.92	–	–
	$\theta_2$	0.99	0.99	0.99	0.99	0.99	–	–
Carbon dioxide	$n_{\text{eq}}$	6.27	6.29	6.31	6.29	6.17	6.12	–
	$\theta_1$	0.72	0.71	0.70	0.71	0.77	0.79	–
	$\theta_2$	0.98	0.98	0.98	0.98	0.99	0.99	–

Note:  $n_{\text{eq}}$  is the hydrate number on the line of three-phase equilibrium at setting the degree of filling of large cavities equal to one;  $\theta_1$  and  $\theta_2$  are the degree of filling of small and large cavities in the hydrate structure, respectively.

spheric pressure (Figs. 3 and 4). It is significant that  $a_{\text{eq}}$  is a function of temperature. This means that for practical application of relations (6), (7) and (8) it is necessary to establish the relationship between  $a_{\text{eq}}$  and temperature. Such a relationship is given in the express method for calculating unfrozen water [Istomin et al., 2017a]:

for temperature in Kelvin

$$-RT \ln a_{\text{eq}} = 6008 \left( 1 - \frac{T}{T_0} \right) - 38.2 \left[ T \ln \frac{T}{T_0} + (T_0 - T) \right] \quad (9)$$

$$(T_0 = 273.15 \text{ K}; T < T_0);$$

for temperature in degrees Celsius

$$a_{\text{eq}} = 1 + 9.6768 \cdot 10^{-3} \cdot t_{\text{eq}} + 4.1769 \cdot 10^{-5} \cdot t_{\text{eq}}^2. \quad (10)$$

Equation (10) can be reversed, i.e., expressed as a relationship between temperature ( $t$ ) (in degrees Celsius) and pore water activity  $a_{\text{eq}}$  on the equilibrium line pore water ice at atmospheric pressure:

$$t_{\text{eq}} = 103.25 \ln a_{\text{eq}} + 5.57 (1 - a_{\text{eq}})^2. \quad (11)$$

### Practical applications of thermodynamic relations for calculation of nonclathrated water content

In practical calculations of nonclathrated water content in the soil system and temperatures above  $0^\circ\text{C}$  it is recommended to use formulas (2), (3) and (4). The calculation scheme is as follows. The soil system is considered, for which it is necessary to calcu-

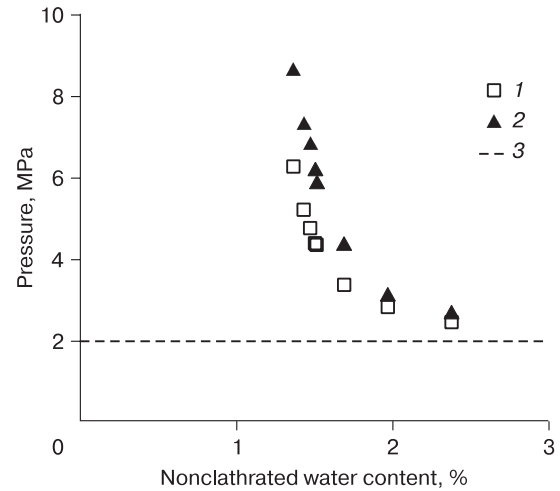


Fig. 4. Effect of methane pressure on the change in the content of nonclathrated water in kaolinite clay at a temperature of  $-7.5^\circ\text{C}$ .

1 – calculated data; 2 – experimental data; 3 – equilibrium pressure “ice–methane–hydrate” at a given temperature [Sergeeva et al., 2021].

late the content of nonclathrated water, the gas-hydrate-forming agent is selected and the temperature is set. The dependence of water activity on sample moisture content (at atmospheric pressure) is determined experimentally. In practice, it is most convenient to use formula (4). As for the hydrate number, in the first approximation it is possible to set its limiting value. Thus, the calculation results in the value of

Table 2. Particle-size distribution and mineralogical composition of soils

Soil	Particle size (mm) distribution, %							Mineralogical composition, %	
	1–0.5	0.5–0.25	0.25–0.1	0.1–0.05	0.05–0.01	0.01–0.002	<0.002		
Sand	0.2	35.7	62.9	0.8	0.3	0.1	–	Quartz	>90
Kaolinite clay	0.7	0.5	0.4	2.9	19.5	34.0	42.0	Kaolinite	92
								Quartz	6
								Muscovite	2

sample moisture content ( $W$ ) (i.e., nonclathrated water content) as a function of vapor pressure ( $P$ ) at the considered temperature.

At the same time, for calculations of nonclathrated water content in the soil system at subzero temperatures, it is recommended to apply a similar algorithm, but use formulas (6), (7) or (8), with  $a_{eq}$  determined by any of relations (9), (10), (11).

It is important to note that by knowing the pore water activity, it is possible to calculate the nonclathrated water content for different hydrate forming gases. An additional consideration here will be the calculation of gas solubility in water ( $x$ ), but the solubility of gases in pore water can be largely neglected, with the exception of  $CO_2$  (due to high solubility) and nitrogen (due to high hydrate formation pressure).

The thermodynamic relations considered above can be used in practice also in the case when the pore water activity was not determined experimentally, but the curve of unfrozen water content for the ground medium was previously obtained by any other method (i.e. the relationship between moisture content and subzero temperature is set). Then, at the first step, the relationship between  $t$  and  $a_{eq}$  is established by formula (10), thus determining the functional dependence of the sample moisture content ( $W$ ) and pore water activity. Knowing  $a_{eq}$ , it is possible to calculate the pressure dependence of nonclathrated water according to the above scheme.

Using formulas (6) and (7), one can also reliably extrapolate experimental data on nonclathrated water to higher pressures. For example, let an experimental point for the investigated soil is obtained for the nonclathrated water content  $W$  at a given tempe-

rate and pressure  $P_1$  by the direct contact method [Chuvilin et al., 2011], and the unfrozen water curve is already available for this soil. Then this experimental point is taken as a reference point, and  $a_1$  is calculated from the curve of unfrozen water by  $W$ . Then, from formulas (6) or (7), by replacing  $P_{eq}^{icc}$  by  $P_1$  and  $a_{eq}$  by  $a_1$ , we obtain an extrapolation formula for calculating the nonclathrate water content for higher values of the pressure of the hydrate-forming gas.

The calculated values of hydrate numbers for different gases on the lines of three-phase equilibria are given below (the calculation was performed using the software HydroFLASH, Hydrafact Ltd) (Table 1).

According to the above-mentioned methodology, the dependence of nonclathrated water content on pressure in samples of kaolinite clay and sand-clay mixtures (sand with 14% kaolinite clay and sand with 25% kaolinite clay) at  $-7.5^\circ C$  was evaluated. Characteristics of soils are presented in Table 2.

The unsalted sand (salinity less than 0.01%) consists of quartz (more than 90%), the predominant fraction of sand particles 0.1–0.25 mm reaches 62.9%. Kaolinite clay consists mainly of kaolinite (92%) with 95.5% silty-clay coarseness, with the percentage of clay particles (<0.002 mm) reaching 42%. Kaolinite clay contains insignificant amount of dissolved salts (0.04%). The specific active surface area of sand and kaolinite clay determined by nitrogen adsorption is 0.2 and 12 m<sup>2</sup>/g, respectively.

To determine the nonclathrated water content of the soils of interest, the experimental dependence of pore water activity ( $a$ ) on the weight moisture content ( $W$ ) of the sample at atmospheric pressure is required (Tables 3 and 4).

Table 3. Experimental data on the change in pore water activity ( $a$ ) in kaolinite clay, when its moisture content  $W$  decreases at 25°C

$W$ , %	$a$	$W$ , %	$a$	$W$ , %	$a$
28.86	0.995	6.41	0.972	2.20	0.897
21.80	0.993	5.42	0.967	1.81	0.866
17.70	0.990	5.12	0.963	1.53	0.830
16.72	0.990	4.07	0.953	1.45	0.813
12.47	0.986	3.55	0.943	1.25	0.753
8.15	0.978	2.79	0.924	1.18	0.720

Table 4. Experimental data on pore water activity  $a$  in sandy-clay mixtures as a function of their moisture content  $W$  at 25°C

Composition of sand-clay mixtures	$W$ , %	$a$
Sand + 14% kaolinite clay	0.70	0.9494
	0.42	0.9229
	0.29	0.8874
	0.17	0.7822
Sand + 25% kaolinite clay	0.84	0.9411
	0.61	0.9065
	0.43	0.8604
	0.31	0.7645

The pore water activity ( $a$ ) was determined on a WP4-T instrument according to the method described in detail above [Chuvilin *et al.*, 2020, 2022].

The equilibrium pressure was then calculated for each pore water activity value using formula (4). This pressure will correspond to the value of moisture content ( $W$ ), which represents the nonclathrated water content. Comparison of the calculated data of nonclathrated water content in kaolinite clay with direct experimental data obtained by contact method is shown in Fig. 4. There is a good agreement between the calculated thermodynamic relations and the experimental data of nonclathrated water content in kaolinite clay obtained by the contact method. The accuracy of the contact method is estimated to be  $\sim 0.1\%$ , and the largest discrepancy of  $\sim 0.15\%$  is observed in the range of nonclathrated water content of 1.4–1.7%.

For sand-clay mixtures consisting of quartz sand and admixture of 14% and 25% kaolinite clay the calculated and experimental data on nonclathrated water content are presented in Fig. 5. These data also show a good agreement between the calculated and experimental parameters of nonclathrated water content. In the model soil media, there is a regular increase in the amount of nonclathrated water with increasing weight content of clay particles. Thus, the content of nonclathrated water at vapor pressure of 4 MPa in sand with kaolinite clay content of 14% is 0.25%, which is two times lower than in sand with clay content of 25%. The effect of vapor pressure on the nonclathrated water content is weakly pronounced at pressures above 6–8 MPa. However, the regular difference in the content of nonclathrated water depending on the content of clay particles remains even under these conditions.

## CONCLUSIONS

The paper presents analytical dependencies for calculating the nonclathrated water content in a soil system at a given temperature depending on the pressure of hydrate-forming gas.

Qualitative regularities of the influence of vapor pressure on nonclathrated water content at both positive and subzero temperatures have been revealed (with increasing pressure the content of nonclathrated water sharply decreases). With the use of the obtained dependences, a method of thermodynamic calculation of the content of nonclathrated water in the sample from the pressure of hydrate-forming gas at a fixed temperature was developed. For its practical realization it is necessary to have data on pore water activity from water content in the sample, or data on the of unfrozen water content in the range of subzero temperatures.

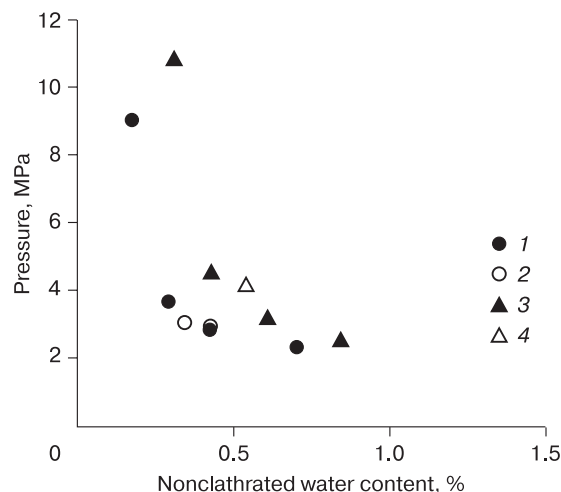


**Fig. 5. Effect of methane pressure on the change in the content of nonclathrated water in sand-clay mixtures at a temperature of  $-5^{\circ}\text{C}$  and an equivalent pressure for methane  $P_{\text{eq}} = 2.36$  MPa.**

1, 3 – calculated data; 2, 4 – experimental data [Sergeeva *et al.*, 2021]; 1, 2 – sand with 14% kaolinite clay; 3, 4 – sand with 25% kaolinite clay.

On the basis of the proposed methodology, calculations of nonclathrated water content in kaolinite clay and sandy-clay mixtures at temperatures below  $0^{\circ}\text{C}$  and methane pressures from about 2.3 MPa to 11 MPa have been carried out. The results obtained by the proposed experimental-calculation method showed a fairly good coincidence with the data of direct determinations by the experimental (contact) method. For the investigated range of pressures, the content of nonclathrated water decreases more than twice with pressure increase, and the greatest change in the content of nonclathrated water is observed at pressures 2–3 MPa higher than the values of equilibrium pressure.

The proposed methodology for estimation of nonclathrated water content in soil and samples containing methane hydrate can be used for other hydrate-forming gases and various dispersed sediments.

The performed methodological developments can be used in assessing the efficiency of methane hydrate extraction from gas hydrate deposits by various technological methods. Data on the content of nonclathrated water in hydrate-saturated reservoirs are also essential for predicting the efficiency of  $\text{CO}_2$  burial in hydrate form.

**Acknowledgements.** The work was financially supported by the Russian Science Foundation, grant nos. 21-77-10074 and 22-17-00112.

## References

- Anderson R., Llamedo M., Tohidi B., Burgass R.W., 2003. Experimental measurement of methane and carbon dioxide clathrate hydrate equilibria in mesoporous silica. *J. Phys. Chem. B.* **107**, 3507–3514.
- Azimi A., Javanmardi J., Mohammadi A.H., 2021. Development of thermodynamic frameworks for modeling of clathrate hydrates stability conditions in porous media. *J. Mol. Liq.* **329**, 115463. DOI: 10.1016/j.molliq.2021.115463
- Chen L.T., Sun C.Y., Chen G.J., Nie Y.Q., 2010. Thermodynamics model of predicting gas hydrate in porous media based on reaction-adsorption two-step formation mechanism. *Ind. Eng. Chem. Res.* **49**, 3936–3943. DOI: 10.1021/ie901878p
- Chong Zh.R., Yang M., Khoo B.Ch., Linga P., 2016. Size effect of porous media on methane hydrate formation and dissociation in an excess gas environment. *Ind. Eng. Chem. Res.* **55**, 7981–7991. DOI: 10.1021/acs.iecr.5b03908
- Chuvilin E.M., Bukhanov B.A., Mukhametdinova A.Z. et al., 2022. Freezing point and unfrozen water contents of permafrost soils: Estimation by the water potential method. *Cold Reg. Sci. Technol.* 196, 103488. DOI: 10.1016/j.coldregions.2022.103488/
- Chuvilin E.M., Gureeva O.M., Istomin V.A., Safonov S.S., 2008. Experimental method for determination of the residual equilibrium water content in hydrate-saturated natural sediments. In: *Proc. 6<sup>th</sup> Int. Conf. on Gas Hydrates (ICGH 2008) (Vancouver, 6–10 July 2008)*. Vancouver, BC, Canada, p. 5490.
- Chuvilin E.M., Istomin V.A., 2012. Temperature dependence of the equilibrium pore water content in gas hydrate contained sediments. In: *Proc. 10<sup>th</sup> Int. Conf. on Permafrost (Salekhard, June 25–29, 2012)*. Yamal-Nenets Autonomous District, Russia, 2012, vol. 2, p. 57–60.
- Chuvilin E.M., Istomin V.A., Bukhanov B.A., 2018. *Method for Determining the Content of Unfrozen Water in Frozen Soils*. Patent RU 2654832 C1. Russian Federation: MPK G01N 25/56 (2006.01). Patent Holder Skolkovo Institute of Science and Technology, 2018. No. 2017121829. Claimed June 21, 2017. Publ. May 22, 2018. Bull. no. 15. (in Russian)
- Chuvilin E.M., Istomin V.A., Safonov S.S., 2010a. *Method for Determining the Content of Pore Water in Equilibrium with Gas Hydrate in Dispersed Media (Variants)*. Patent RU 2391650 C1. Russian Federation: MIIK G01N 25/00 (2006.01). Patent Holder Schlumberger Technology B.V. (NL), 2010. No. 2008148000/28. Claimed December 5, 2008. Publ. June 10, 2010. Bull. No. 16. (in Russian)
- Chuvilin E.M., Istomin V.A., Safonov S.S., 2010b. Method for Determination of Pore Water Content in Equilibrium with Gas Hydrate in Dispersed Media: Patent US 2010/0139378 A1.; Publ. 10, June 2010.
- Chuvilin E.V., Istomin V.A., Safonov S.S., 2011. Residual non-clathrate water in sediments in equilibrium with gas hydrate, comparison with unfrozen water. *Cold Reg. Sci. Technol.* **68**, 68–73. DOI: 10.1016/j.coldregions.2011.05.006
- Chuvilin E.M., Sokolova N.S., Bukhanov B.A. et al., 2020. Application of water potential method for unfrozen water content determination in different frozen soils. *Earth's Cryosphere XXIV* (5), 14–22.
- Clarke M.A., Pooladi-Darvish M., Bishnoi P.R., 1999. A method to predict equilibrium conditions of gas hydrate formation in porous media. *Ind. Eng. Chem. Res.* **38**, 2485–2490. DOI: 10.1021/ie980625u
- Em Y., Stoporev A., Semenov A. et al., 2020. Methane hydrate formation in halloysite clay nanotubes. *ACS Sustain. Chem. Eng.* **8**, 7860–7868. DOI: 10.1021/acssuschemeng.0c00758
- Handa Y.P., Stupin D.Y., 1992. Thermodynamic properties and dissociation characteristics of methane and propane hydrates in 70-ANG-radius silica gel pores. *J. Phys. Chem.* **96**, 8599–8603. DOI: 10.1021/j100200a071
- Hansen T.C., Falenty A., Kuhs W.F., 2016. Lattice constants and expansivities of gas hydrates from 10 K up to the stability limit. *J. Chem. Phys.* **144**, 054301.
- Istomin V.A., Chuvilin E.M., Bukhanov B.A., 2015a. Phase equilibria pore water–gas phase–bulk gas hydrates or ice. In: *Int. Conf. on Functional Materials for Frontier Energy Issues (Novosibirsk, 1–5 Oct., 2015)*. Novosibirsk, p. 10.
- Istomin V.A., Chuvilin E.M., Bukhanov B.A., 2015b. Evaluation of equilibrium water content in hydrate saturated porous media. In: *EAGE. Geomodel. (Gelendzhik, Sept. 7–10, 2015)*. Gelendzhik, p. 1–5. (in Russian)
- Istomin V.A., Chuvilin E.M., Bukhanov B.A., 2017a. Fast estimation of unfrozen water content in frozen soils. *Earth's Cryosphere XXI* (6), 116–120.
- Istomin V.A., Chuvilin E.M., Bukhanov B.A., Uchida T., 2017b. Pore water content in equilibrium with ice or gas hydrates in sediments. *Cold Reg. Sci. Technol.* **137**, 60–67. DOI: 10.1016/j.coldregions.2017.02.005/
- Istomin V.A., Chuvilin E.M., Makhonina N.A., Bukhanov B.A., 2009. Temperature dependence of unfrozen water content in sediments on the water potential measurements. *Kriosfera Zemli XIII* (2), 35–43. (in Russian)
- Istomin V.A., Chuvilin E.M., Sergeeva D.V. et al., 2018. Influence of composition and external gas pressure on ice and hydrate formation in gas-saturated pore solutions. *Neftegazokhimiya* **2**, 33–42. (in Russian)
- Istomin V.A., Yakushev V.S., 1992. *Natural Gas Hydrates*. Moscow, Nedra, 236 p. (in Russian)
- Kang S.P., Lee J.W., Ryu H.J., 2008. Phase behavior of methane and carbon dioxide hydrates in meso- and macro-sized porous media. *Fluid Phase Equilib.* **274**, 68–72. DOI: 10.1016/j.fluid.2008.09.003
- Klauda J.B., Sandler S.I., 2001. Modeling gas hydrate phase equilibria in laboratory and natural porous media. *Ind. Eng. Chem. Res.* **40**, 4197–4208. DOI: 10.1021/ie000961m
- Lee S., Seo Y., 2010. Experimental measurement and thermodynamic modeling of the mixed CH<sub>4</sub> + C<sub>3</sub>H<sub>8</sub> clathrate hydrate equilibria in silica gel pores: Effects of pore size and salinity. *Langmuir* **26**, 9742–9748. DOI: 10.1021/la100466s
- Li X.S., Zhang Y., Li G. et al., 2008. Gas hydrate equilibrium dissociation conditions in porous media using two thermodynamic approaches. *J. Chem. Thermodyn.* **40**, 1464–1474. DOI: 10.1016/j.jct.2008.04.009
- Liang W., Zhou J., Wei C., 2021. Uniqueness of the equilibrium relationship among temperature, pressure and liquid water content in hydrate-bearing soils. *J. Nat. Gas Sci. Eng.* **88**, 103820. DOI: 10.1016/j.jngse.2021.103820
- Liu H., Zhan S., Guo P. et al., 2018. Understanding the characteristic of methane hydrate equilibrium in materials and its potential application. *Chem. Eng. J.* **349**, 775–781. DOI: 10.1016/j.cej.2018.05.150
- Makogon Yu.F., 1974. *Hydrates of Natural Gases*. Moscow, Nedra, 208 p. (in Russian)
- Melnikov V.P., Nesterov A.N., 2001. Gas hydrate formation from porous mineralized water. *Kriosfera Zemli V* (1), 61–67. (in Russian)
- Melnikov V.P., Nesterov A.N., Reshetnikov A.M. et al., 2010. Stability and growth of gas hydrates below the ice–hydrate–gas equilibrium line on the P–T phase diagram. *Chem. Eng. Sci.* **65** (2), 906–914.

- Melnikov V.P., Nesterov A.N., Reshetnikov A.M., Istomin V.A., 2011. Metastable states during dissociation of carbon dioxide hydrates below 273 K. *Chem. Eng. Sci.* **66** (1), 73–77.
- Park T., Lee J.Y., Kwon T.H., 2018. Effect of pore size distribution on dissociation temperature depression and phase boundary shift of gas hydrate in various fine-grained sediments. *Energy Fuels* **32**, 5321–5330. DOI: 10.1021/acs.energyfuels.8b00074
- Sell K., Quintal B., Kersten M., Saenger E.H., 2018. Squirt flow due to interfacial water films in hydrate bearing sediments. *Solid Earth* **9**, 699–711.
- Seo Y., Lee H., Uchida T., 2002. Methane and carbon dioxide hydrate phase behavior in small porous silica gels: Three-phase equilibrium determination and thermodynamic modeling. *Langmuir* **18**, 9164–9170. DOI: 10.1021/la0257844
- Sergeeva D., Istomin V., Chuvilin E. et al., 2021. Influence of hydrate-forming gas pressure on equilibrium pore water content in soils. *Energies* **14** (7), 1841. DOI: 10.3390/en14071841
- Smith D.H., Wilder J.W., Seshadri K., 2002. Methane hydrate equilibria in silica gels with broad pore-size distributions. *AICHE J.* **2**, 393–400.
- Smith D.H., Seshadri K., Uchida T., Wilder J.W., 2004. Thermodynamics of methane, propane, and carbon dioxide hydrates in porous glass. *AICHE J.* **7**, 1589–1598. DOI: 10.1002/aic.10141
- Uchida T., Ebinuma T., Ishizaki T., 1999. Dissociation condition measurements of methane hydrate in confined small pores of porous glass. *J. Phys. Chem. B.* **103**, 3659–3662.
- Uchida T., Ebinuma T., Takeya S. et al., 2002. Effects of pore sizes on dissociation temperatures and pressures of methane, carbon dioxide and propane hydrate in porous media. *J. Phys. Chem. B.* **106**, 820–826. DOI: 10.1021/jp012823w
- Uchida T., Takeya S., Chuvilin E.M. et al., 2004. Decomposition of methane hydrates in sand, sandstone, clays and glass beads. *J. Geophys. Res.* **109**, B05206. DOI: 10.1029/2003JB002771
- Wilder J.W., Seshadri K., Smith D.H., 2001. Modeling hydrate formation in media with broad pore size distributions. *Langmuir* **17**, 6729–6735.
- Yakushev V.S., 2019. Experimental modeling of methane hydrate formation and decomposition in wet heavy clays in Arctic regions. *Geosciences* **9**, 13.
- Zarifi M., Javanmardi J., Hashemi H. et al., 2016. Experimental study and thermodynamic modelling of methane and mixed C<sub>1</sub> + C<sub>2</sub> + C<sub>3</sub> clathrate hydrates in the presence of mesoporous silica gel. *Fluid Phase Equilibria* **423**, 17–24. DOI: 10.1016/j.fluid.2016.03.018
- Zaripova Y., Yarkovoi V., Varfolomeev M. et al., 2021. Influence of water saturation, grain size of quartz sand and hydrate-former on the gas hydrate formation. *Energies* **14**, 1272. DOI: 10.3390/en14051272
- Zhang Y., Taboada-Serrano P., 2020. Model for gas-hydrate equilibrium in porous media that incorporates pore-wall properties. *Phys. Chem. Chem. Phys.* **22**, 10900–10910. DOI: 10.1039/D0CP01263G
- Zhou J., Liang W., Wei C., 2019. Phase equilibrium condition for pore hydrate: Theoretical formulation and experimental validation. *J. Geophys. Res. Solid Earth* **124**, 12703–12721. DOI: 10.1029/2019JB018518

Received January 30, 2024

Revised May 27, 2024

Accepted June 23, 2024

Translated by E.S. Shelekhova